HHS Public Access

Author manuscript

J Orthop Res. Author manuscript; available in PMC 2023 February 01.

Published in final edited form as:

J Orthop Res. 2022 February ; 40(2): 348–358. doi:10.1002/jor.25050.

Painful temporomandibular joint overloading induces structural remodeling in the pericellular matrix of that joint's chondrocytes

Melissa Franklin[1], **Megan Sperry**[2,*], **Evan Phillips**[3], **Eric Granquist**[4], **Michele Marcolongo**[3], **Beth A. Winkelstein**[2]

[1]School of Biomedical Engineering, Science, and Health Systems, Drexel University, Philadelphia, PA, 19104

[2]Department of Bioengineering, University of Pennsylvania, Philadelphia, PA, 19104

[3]Department of Materials Science and Engineering, Drexel University, Philadelphia, PA 19104

[4]Oral & Maxillofacial Surgery, University of Pennsylvania, Philadelphia, PA 19104

Abstract

Mechanical stress to the TMJ is an important factor in cartilage degeneration, with both clinical and pre-clinical studies suggesting that repeated TMJ overloading could contribute to pain, inflammation, and/or structural damage in the joint. However, the relationship between pain severity and early signs of cartilage matrix microstructural dysregulation is not understood, limiting advancement of diagnoses and treatments for TMJ-OA. Changes in the pericellular matrix (PCM) surrounding chondrocytes may be early indicators of osteoarthritis. A rat model of TMJ pain induced by repeated jaw loading (1 hr/day for 7 days) was used to compare the extent of PCM modulation for different loading magnitudes with distinct pain profiles (3.5N – persistent pain, 2N – resolving pain, or unloaded controls – no pain) and macrostructural changes previously indicated by Mankin scoring. Expression of PCM structural molecules, collagen VI and aggrecan NITEGE neo-epitope, were evaluated at day 15 by immunohistochemistry within TMJ fibrocartilage and compared between pain conditions. Pericellular collagen VI levels increased at day 15 in both the 2N ($p=0.003$) and 3.5N ($p=0.042$) conditions compared to unloaded controls. PCM width expanded to a similar extent for both loading conditions at day 15 (2N, $p<0.001$; 3.5N, $p=0.002$). Neo-epitope expression increased in the 3.5N group over levels in the 2N group ($p=0.041$), indicating pericellular changes that were not identified in the same groups by Mankin scoring of the pericellular region. Although remodeling occurs in both pain conditions, the presence of pericellular catabolic neo-epitopes may be involved in the macrostructural changes and behavioral sensitivity observed in persistent TMJ pain.

[*]Corresponding Author(s): Megan Sperry, PhD, Wyss Institute at Harvard University, 3 Blackfan Circle, Boston, MA 02115, megan.sperry@wyss.harvard.edu, 978-387-3763.

Author Contributions Statement:

MF and MS developed the approach and designed the experiments. MF implemented the experiments, performed analyses, and interpreted data with supervision from MS. EP developed protocols for data analysis and assisted with data interpretation. EG helped supervise project, provided a clinical framework and funding support. MM and BAW conceived and guided the original project ideas and provided funding support. MF wrote the manuscript with support and editing from MS, MM, and BAW. All authors discussed the results and provided critical feedback that shaped the research and the manuscript.

Declaration of Conflict of Interest:

Dr. Granquist is a consultant for Zimmer Biomet but has no conflict. The authors declare no potential conflicts of interest with respect to the authorship and/or publication of this article.

Graphical Abstract

The pericellular matrix (PCM) reorganizes following repeated TMJ overloading in a rat model with tunable pain conditions. There is subtle expansion of pericellular width, and increased expression of aggrecan neo-epitope and collagen VI. Collagen VI increases independent of loading magnitude whereas aggrecan fragmentation increases upon greater loading. Here, we characterize the dynamic microenvironment of the PCM and begin to bridge the complex relationships between pain, cartilage biochemical changes, and structural degradation representative of progressive TMJ-OA.

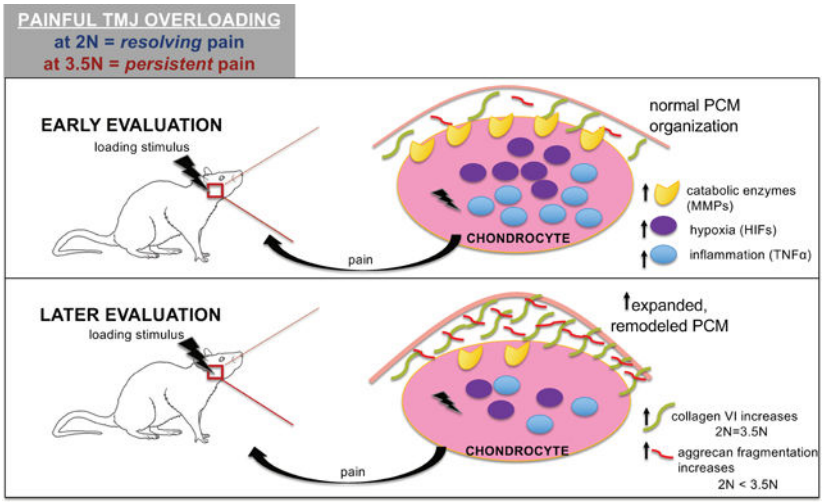

Keywords

pericellular matrix; temporomandibular joint; osteoarthritis; joint overloading; collagen

Introduction

Temporomandibular joint disorders (TMDs) are the second-most common source of orofacial pain[1]. A substantial subset of patients with TMD develop osteoarthritis (OA), which is characterized by intra-articular inflammation and cartilage degeneration[2]. Macroscopic changes observed with TMJ-OA include changes in joint shape and size, decreased condylar cartilage volume, and thickened articular disc and surrounding fossa[3,4]. There is a known association between osteoarthritic related symptomatic pain and tissue degeneration[2, 5, 6–8]. However, differential diagnoses and treatments for patients experiencing latent pain and those who develop chronic, active orofacial pain remain a clinical challenge. Accordingly, studying the relationship between pain and changes in tissue structure that are characteristic of TMJ-OA is needed.

Osteoarthritis pathology involves alteration in the catabolic, inflammatory, and structural molecular components of the condylar cartilage tissue, which consists of chondrocytes[2, 5, 9, 10]. The pericellular matrix (PCM) surrounds chondrocytes within the temporomandibular condyle and plays an important role in mechanotransduction, cytoprotection, and biochemical signaling[10–13]. The PCM consists of densely packed

collagens and proteoglycans, including collagen VI and aggrecan, each with critical roles in maintaining the PCM's structural integrity. Collagen VI serves as a mechanical tether and protective layer surrounding chondrocytes[14,15], whereas aggrecan is primarily responsible for regulating hydration, swelling, and supporting compression[16–19] (Figure 1B). Recently, PCM microstructural changes have been suggested to compromise chondrocyte mechanical properties[20] and serve as early indicators for osteoarthritis progression[21].

The structural and morphological changes associated with osteoarthritic cartilage are often assessed by the well-established Mankin grading system[22]. That technique evaluates the overall health of the cartilage tissue using grading of the intensity of histologically stained cartilage, including categorizing the label intensity of the PCM[23,24]. Although accepted as a reliable tool to study TMJ-OA[22–24], there are constraints with Mankin scoring not being able to provide a detailed view of histological outcomes, especially within localized regions like the dynamic pericellular matrix[21,26]. In experimental models of OA that target specific markers within the PCM, there is evidence that collagen VI levels increase and become more distributed throughout the tissue matrix[27,28]. It is also well accepted that aggrecan depletion is characteristic of osteoarthritic development in other joint models[16–18,29–32]. Together, organizational changes in collagen VI and aggrecan biomarkers destabilize the PCM and contribute to onset of OA and mediate disease severity[29, 33,34]. Further, while the Mankin score remains popular for its adaptability to several animal species and human cartilage models[22], the scoring system's accuracy has not been compared to use of pericellular marker labelling to detect early TMJ-OA progression.

This study sought to evaluate the extent of pericellular structural modulation in the TMJ using a tunable rat model of temporomandibular joint pain that is induced by repeated loading of the jaw (Figure 1A) and that has been well-characterized for its painful behavioral outcomes, as well as inflammatory and catabolic cascades representative of TMJ-OA pathomechanisms[2, 25, 35,36]. Previous work with this model graded orofacial expression through the Rat Grimace Scale (RGS) to score affective TMJ pain and mechanical reflex responses defining a threshold for evoked peripheral sensitivity[25]. Briefly, a 2N load of repeated mouth-opening induces resolving pain whereas a greater 3.5N of force induces persistent pain behaviors[2, 25,36] (Figure 1A). Further, TMJs from both loading paradigms were previously characterized by the Mankin scoring system and only the 3.5N-loaded persistent pain condition was found to exhibit significant tissue structural changes at day 15[25]. In the present study, changes in the pericellular collagen VI protein and aggrecan NITEGE neo-epitope were evaluated at day 15 for both the resolving and persistent pain conditions.

Our central hypothesis is that collagen VI and aggrecan neo-epitope expression and distribution will increase in painful, overloaded TMJs compared to unloaded controls, with the greatest extent of pericellular remodeling occurring in TMJs that develop persistent sensitivity. Collagen VI is expected to increase since chondrocytes upregulate protein synthesis to preserve pericellular matrix tethering and protect against further degradation. Furthermore, we expect increased aggrecan fragmentation (i.e., expression of neo-epitope) in the TMJ cartilage since it is an initial indication of degradation and subsequent proteoglycan loss characteristic of OA. Characterizing PCM molecule expression and

distribution will help identify whether there is degradation and provide detailed insight into the tissue structural outcomes of TMJ-OA. In addition, this investigation begins to define a relationship between a painful mechanical overloading paradigm and pericellular changes characteristic of TMJ-OA onset and progression.

Methods

Mechanical Loading of Rat TMJ

All studies used adult, weight-matched (277.50±4.24 g) and age-matched (70–80 days following receipt) female Holtzman rats (Envigo; Indianapolis, IN). Rats were housed in groups of 2–3 in standard polycarbonate caging (AnCare; Bellmore, NY), with 0.25-inch corncob bedding (Bed-o'Cobs; The Andersons Lab Bedding Products; Maumee, OH) and ad libitum access to food (LabDiet 5001; LabDiet; St Louis, MO) and water (acidified to pH = 3). Rats were housed in an Association for Assessment and Accreditation of Laboratory Animal Care accredited vivarium under a 12:12 hour light:dark cycle in a temperature-controlled environment in accordance with recommendations set forth in The Guide for Care and Use of Laboratory Animals (8th edition)[37]. All animal procedures were approved by the IACUC at the University of Pennsylvania (IACUC #803831) and adhered to research and ethical guidelines of the International Association for Study of Pain[38]. Rats were exposed in separate, randomized groups to daily repeated mechanical loading of the jaw under isoflurane anesthesia at 2N (induces resolving orofacial sensitivity) and 3.5N (induces persistent orofacial sensitivity) for 1 hour each day for 7 days[2, 25, 36] (Figure 1A). All mechanically loaded TMJs were compared to control TMJs from rats that did not receive loading (normal). For all tissue harvests, rats were deeply anesthetized with pentobarbital (65 mg/kg) and perfused with phosphate buffer saline (PBS).

TMJ Behavioral Sensitivity Assessment

Mechanical reflex testing in the temporomandibular joint region was used to determine the extent of temporomandibular pain for each loading magnitude. Joint sensitivity reflex tests were performed at baseline (before loading), every other day during (days 1, 3, 5), and after the loading period (days 7, 9, 11, 13, and 14) for rats exposed to 2 or 3.5N loading. Sensitivity measurements were acquired in the morning prior to that day's loading. The threshold for eliciting a head withdrawal was measured using von Frey filaments of increasing strengths from 0.6 to 60 g to stimulate the TMJ region (Stoelting, Wood Dale, IL)[39]. This assessment for pain sensitivity was performed on the subset of rats used for the day 15 pericellular structural assays in this study (n=7/group). A separate analysis compared the 3.5N-loaded animals in the day 8 and day 15 tissue groups (n=5/group). Head withdrawal thresholds were averaged across each group, log-transformed to normalize distribution, then compared used a repeated-measures analysis of variance with a post-hoc Sidak's multiple comparisons test (α=0.05)[2,25,36].

TMJ Tissue Preparation

To assess collagen VI expression, rats from the no loading, 2N, and 3.5N groups (n=5/group) were fixed by 4% paraformaldehyde and TMJs were harvested en bloc at day 15. All fixed TMJs were stored in 30% sucrose in PBS and later decalcified with 0.25M EDTA

for 3 weeks at 4°C. A separate set of fixed TMJs (n=5 rats) were also harvested at day 8 from the 3.5N loading condition. To assess aggrecan NITEGE neo-epitope expression, TMJs were harvested un-fixed freshly from the no loading, 2N, and 3.5N groups at day 15 (n=4 rats/group), immediately placed in 10% protease inhibitor cocktail in PBS to avoid protein degradation and stored at −20°C. Table 1 summarizes the experimental groups and assessments completed in this study.

Immunohistochemistry and Immunofluorescence Labelling

Fixed TMJs were embedded in Tissue–Tek OCT compound (Saukura Finetek; Torrance, CA) and sagittally sectioned. Fixed TMJ sections used for immunohistochemistry (IHC) were sectioned at 18μm, and thaw-mounted onto slides. IHC was performed via incubating sections with primary antibody against collagen VI (1:1250; Fitzgerald; Acton, MA) or aggrecan NITEGE neo-epitope (1:1000; Thermo Fisher; Waltham, MA) overnight at 4°C. After washing, sections were incubated with biotinylated horse anti-rabbit secondary (1:1,000; Vector Laboratories; Burlingame, CA) for 2 hours, developed using 3,3-diamimobenzidine (DAB), and cover-slipped. For collagen VI expression assessment, two histological sections of each DAB-IHC TMJ sample were imaged at 40x using the EVOS FL Auto Imaging System (Thermo Fisher Scientific; Waltham, MA). Fresh TMJs used for immunofluorescence evaluation were similarly embedded, then sectioned at 5μm with direct adherence to Kawamoto's sectioning tape. Sections were incubated for 30 minutes at room temperature using the same primary antibodies with higher concentrations (1:50 and 1:25 for collagen VI and NITEGE neo-epitope respectively). The secondary label was then applied to sections for 30 minutes using goat anti-rabbit AlexaFlour 488. For aggrecan neo-epitope expression assessment, two histological sections of each IF-IHC labelled TMJ were imaged using confocal microscopy (Leica® TCS SP8 Multiphoton Confocal; 63x magnification; 15% laser intensity, 850V gain).

Quantification of Pericellular Marker Expression

Collagen VI expression was quantified using DAB-IHC images. Images were cropped to an approximated depth within the fibrocartilage tissue (150–200μm)[29] and at standardized image dimensions (1000 × 500 pixels) to include the deep-hypertrophic zone. This zone was selected for analysis because it is proteoglycan-rich, and since resistance to compression is largely dictated by proteoglycan-collagen networks, this region is suggested to show a stronger response to applied loads[40] and cause the earliest mechanical matrix imbalances associated with TMJ-OA compared to the superficial, fibrous layers[41–43]. A custom MATLAB script measured collagen VI expression as a percentage of surface area[44]. Following percent positive pixels analysis of collagen VI expression for each experimental group and unloaded controls, an additional average PCM width analysis was performed manually to quantify extent of pericellular expansion following loading conditions using ImageJ with collagen VI as guidance marker (Figure 1C). Width measurements were derived from the MATLAB-processed, bi-filtered images and were taken at a perpendicular angle from the inner-most boundary (interfacing intracellular space) to outer-most boundary (interfacing the extracellular space) of a chondrocyte's PCM ring. Each TMJ sample had two images that underwent PCM width analysis, where the pericellular width was averaged from ten randomized chondrocytes per image.

Aggrecan NITEGE neo-epitope expression was quantified from IF-IHC images cropped to the deep-hypertrophic zone at standardized dimensions (900 × 350 pixels) and the labeled area was measured using the same MATLAB code to calculate the percentage of surface area. Separate one-way ANOVAs and post-hoc Tukey tests (α=0.05) were performed to determine significance for each expression characterization and for PCM width analysis.

Pericellular Mankin Scoring from Safranin-O/Fast Green Histological Images

Global cartilage structure was evaluated using previously published methods[25]. Briefly, TMJs were stained by Safranin-O/Fast Green, imaged by widefield microscopy, and evaluated for the extent of cartilage degradation by two blinded observers using the modified Mankin scale[23,24]. The global Mankin scoring evaluated four subcategories including pericellular and background Safranin-O/Fast Green labelling, chondrocyte arrangement, and structural condition of the cartilage, ranging from a combined score of 0 representing normal cartilage to a maximum of 10 for severely degenerated cartilage totaled from sub-scores from the subcategories[23–25]. This investigation focused on the pericellular sub-category of Mankin scoring to determine if changes in the pericellular structure demonstrated similar trends to that of collagen VI and aggrecan neo-epitope expression levels across loading conditions. The pericellular category ranges from 0 (representing normal) to 2 (representing intensely enhanced Safranin-O/Fast Green pericellular label, indicative of PCM degradation) and contributes to the global Mankin scoring out of 10[23,24]. The two observers' sub-scores of the pericellular category were extracted and averaged. Pericellular Mankin scores were compared between the 2N and 3.5N loading cases at day 15 (n=4 rats/group) by one-way ANOVA and subsequent post-hoc Tukey tests (α=0.05). Pericellular Mankin scores were separately compared between day 8 and day 15 experimental groups of the 3.5N-loaded, persistent pain condition.

Results

Mechanical Reflex Testing Assessment for Behavioral Sensitivity

Head withdrawal thresholds did not differ between the resolving (2N) and persistent (3.5N) pain conditions on days 1, 3, and 5 during the loading period, as well as after the loading period on days 7 and 9 ($p>0.05$) (Figure 2). However, on days 11, 13, and 14 after loading, withdrawal thresholds were higher for the 2N condition, indicating lower TMJ pain sensitivity ($p<0.0001$) (Figure 2). Further, there was no significant difference between the 3.5N-loaded animals with tissue harvested at day 8 and day 15 (Supplemental Figure 2), indicating consistency across groups exposed to 3.5N TMJ overloading.

Collagen VI Expression & Pericellular Width Measurement

The amount of collagen VI increased in 3.5N-loaded TMJs on day 15 (13.59%±2.68%) compared to normal (8.31%±2.66%; p=0.042) (Figure 3). The area percent of collagen VI also increased in 2N-loaded TMJs on day 15 (16.46%±3.60%) compared to normal (p=0.003) (Figure 3). No changes in collagen VI were identified between the 2N and 3.5N load at day 15 (p=0.323). PCM widths, measured with the guidance of collagen VI staining, for 3.5N-loaded TMJs (2.99μm±0.18, p=0.002) and 2N-loaded TMJs (3.28μm±0.44, $p<0.001$) both indicated expansion of pericellular region over normal widths (2.00±0.33)

(Figure 5). Separately, collagen VI expression at an earlier day 8 timepoint within the persistent pain, 3.5N-loaded group was not statistically different than that of unloaded controls (Supplemental Figure 3).

Aggrecan Neo-epitope Expression

The percent positive pixels for NITEGE aggrecan neo-epitope increased in both 2N (13.52% ± 6.74%) and 3.5N (24.29% ± 5.65%) loaded TMJs at day 15 over normal baseline (4.86% ± 1.99%, $p=0.048$ and $p<0.001$ respectively) (Figure 4). Additionally, in contrast to collagen VI expression, there was a significant increase in expression from the 2N-loaded group to the 3.5N-loaded paradigm ($p=0.041$).

Pericellular Mankin Scoring

There were no significant differences of average pericellular Mankin score (out of a possible maximum of 2) identified in the day 15 3.5N-loaded (0.84± 0.71, $p=0.239$) or day 15 2N-loaded TMJs (0.25±0.09, $p=0.999$) compared to normal control TMJs (0.25±0.40) (Figure 6). Additionally, no significant differences in average score were found when comparing the day 15 resolving, 2N-loaded versus persistent, 3.5N-loaded pain models ($p=0.24$) (Figure 6). This corresponds with previously reported average global Mankin scorings (out of a possible maximum of 10) of 4.10±0.37 in day 15, 3.5N-loaded samples, which was greater than that of normal control (1.71 ± 0.64) as well as of the day 15, 2N-loaded TMJ sample group (2.1 ± 0.92)[25]. Within the persistent pain condition, there was no significant difference of pericellular Mankin scores between day 8, 3.5N-loaded TMJ samples compared to normal or day 15 TMJ samples (Supplemental Figure 4).

Discussion

This study identified increased collagen VI (Figure 3) and aggrecan neo-epitope expression by day 15 (Figure 4) in both resolving (2N loaded) and persistent (3.5N loaded) pain behavior conditions of a tunable TMJ overloading model (Figure 2). Collagen VI expression increased in both 2N and 3.5N loaded TMJs by day 15 (Figure 3), and aggrecan neo-epitope expression was increased more extensively within 3.5N loaded samples compared to that of 2N loaded TMJs (Figure 4). Our results show the degree of aggrecan fragmentation may be dependent on overloading magnitude that induce differential pain responses (Figure 4); whereas the increase in collagen VI above normal levels is similar in both loading conditions (Figure 4). This suggests aggrecan fragmentation could be used to differentiate pain responses and severity of biochemical changes characteristic of early TMJ-OA. These findings also suggest that different structural components of the PCM have variable responses to mechanical loading of the TMJ fibrocartilage and some aspects of those microstructural changes are observed even for cases when orofacial pain resolves.

Increases in collagen VI are observed regardless of loading magnitude (Figure 3A). Under normal, non-loaded conditions, collagen VI localizes as thin pericellular rings. In both loading conditions at day 15, the marker appears more densely concentrated within a pericellular region compared to controls as well as more dispersed throughout the peripheral regions of the tissue matrix (Figure 3B). An increase in collagen VI is

thought to be an early defensive mechanism against chondrocyte apoptosis, propagation of the inflammatory response, and catabolic degradation[29,30]. Further, early hypoxia induces upregulation of endoplasmic reticulum (ER) stress markers, causing increased secretion of ER-produced proteins[45] including collagens. Similarly, collagen VI may increase in this model even with early, mild inflammatory and catabolic changes (i.e., within the 2N, resolving pain condition) as a compensatory or preventative mechanism to protect against further degradative responses[27], chondrocyte apoptosis[27–29], or from an alternative pathomechanism[45]. Nugent et al. describes cellular stress and compensatory changes leading to a challenging balance of cellular synthesis, secretion, and localization of pericellular collagen VI with increased dispersion of the protein across the tissue matrix[45]. The finding that there is similar expression of collagen VI in both the 2N and 3.5N loading paradigms at day 15 is particularly interesting since previous work indicated greater expression of MMP-13 at day 7, hypoxia inducible factor (HIF)-1α/HIF2-α catabolic factors by day 8 and tumor necrosis factor (TNF)-α at day 7 only for the greater magnitude (3.5N) loading condition[2, 25, 35,36]. Aligned with recent literature, the increase in collagen VI at day 15 in both 2N and 3.5N loading models could be explained by compensatory phenomena under mild indicators of metabolic stress as well as by biomechanically sensitive chondrocytes attempting to maintain normal tethering to the cartilage ECM via additional secretions when exposed to overloading conditions[14,33,45].

Throughout onset and progression of OA, aggrecan depletion occurs through upregulation of matrix metalloproteinases (MMPs) or aggrecanase (i.e. a disintigrin and metalloproteinase with thrombospondin motifs, ADAMTS family) proteolytic cleavage between the three globular domains of an aggrecan structure[31,32, 46–48]. Prior to full degradation, aggrecan molecules become increasingly fragmented, with the newly cleaved pieces known as neo-epitopes[46,49,50]. The aggrecan NITEGE neo-epitope was selected for assessment since it is the most abundantly accumulated before subsequent total aggrecan loss[46,47]. Moreover, this production of this aggrecan fragment precedes the upregulation of other neo-epitopes such as VDIPEN[47,51] and is directly cleaved by aggrecanases as opposed to MMPs, making it a useful primary marker for early OA. Its accumulation also reveals the presence of ADAMTS-family catabolic factors, which have not been previously characterized in this model[2].

Aggrecan NITEGE neo-epitope levels increased over normal levels by day 15 in both the resolving and persistent pain cases (Figure 4) suggesting that ADAMTS-family aggrecanases activate and affect the structural architecture of the TMJ in pain. However, in contrast to the collagen VI expression results (Figure 3), the neo-epitope levels are greater in the persistently painful 3.5N-loaded group than in the resolving pain 2N-loaded samples (Figure 4A). The progressive increase in expression with increasing loading magnitude is similar to trends observed for MMP-13 and HIF1α/HIF2α catabolic factors at earlier timepoints[2,36]. This similarity of expression related to load magnitude may be evidence of these catabolic factors' influences on aggrecan NITEGE fragmentation in this model. Since these catabolic factors have been shown to regulate the activity of MMP/ADAMTS and subsequent proteoglycan cleavage[2, 31,32, 46–53], these findings suggest that the previously studied catabolic factors may more directly impact the proteolytic cleavage pathway represented in aggrecan neo-epitope expression in comparison to collagen VI

upregulation. Yet, the specific mechanistic pathways that direct the contrasting expression patterns between collagen VI and aggrecan neo-epitope in this model are still unknown.

Aggrecan neo-epitope not only increased with TMJ loading, but also underwent a shift of localization of NITEGE in mechanically loaded TMJ tissue distinct from normal TMJs. In control hypertrophic chondrocytes, the NITEGE neo-epitope was present as pericellular rings as well as intracellular fragments (Figure 4B). In tissue exposed to 2N and 3.5N loading protocols NITEGE is progressively more present and distributed in the pericellular to extracellular matrices (Figure 4B). Other models investigating chondrocyte contents have identified that aggrecan G1 domains are indeed present intracellularly and contribute to intracellular trafficking prior to secretion[54,55]. The difference in localization and distribution between controls and loaded samples could be attributed to stress induced cellular disruption and dysregulated aggrecan catabolism[54]. The upregulation of catabolic activity (evident with MMP-13 and HIFs) and proteolytic cleavage (via ADAMTS) of aggrecan in the loaded models may prevent normal intracellular NITEGE epitope expression and activity. Further, in this increasingly hostile, catabolic microenvironment of the presented models, the chondrocyte and surrounding tissue complex may lose stability and endocytosis capabilities[54]. In turn, the aggrecan neo-epitope fragments become congregated within the pericellular and extracellular matrices[54]. Alternatively, it is possible intracellular aggrecan neo-epitope labelling results from non-specific sticking of antibody to existing intracellular nucleic acids; however, this rationale needs to be explored further by testing different immunohistochemical labelling techniques.

Aggrecan neo-epitope presence in both intracellular and pericellular regions in normal chondrocytes (Figure 4) contrasts with collagen VI localization, which solely appears as pericellular rings (Figure 3). This difference furthers the concept that these two molecular components, although both pivotal to PCM structural integrity, vary in localization, have separate roles throughout the chondron unit and ECM, and may be potentially influenced by differing catabolic pathways. This is not surprising as the two biomarkers are intrinsically different: collagen VI primarily serves as a structural network protein[14,15,33], whereas aggrecan neo-epitope is a degradation product of a proteoglycan protein functioning to retain hydration[16–19]. By establishing unique patterns of pericellular collagens and proteoglycans, we can begin to understand each structure’s properties, potentially informative to each biomolecules’ functions within the PCM. Furthermore, with identifying variable expression trends of these pericellular structures, there is clear evidence of a dynamic and sensitive PCM environment within these painful overloading conditions. These are critical findings because they establish detailed microstructural alterations indicative of early osteoarthritic degeneration and align with human data on pericellular reorganization[56], which highlights the clinical relevance of our model.

This investigation utilized collagen VI to quantify pericellular width expansion, a technique previously cited to determine PCM edges and indicative of the regional structural integrity[33]. The pericellular matrix width results within this overloading model align with collagen VI expression levels within resolving (2N) and persistent (3.5N) conditions by day 15 in that both loaded groups experienced a similar degree of PCM expansion compared to non-loaded controls (Figure 5). Even with evidence of early inflammatory and catabolic upregulation

(day 7/day 8) and subsequent structural reorganization (day 15), our investigation reveals the pericellular expansion is subtle at an average of 3μm for both conditions compared to a normal chondrocyte PCM width average of 2μm and does not exceed 4μm characteristic of advanced, degenerative OA[21]. PCM thickness of less than 4μm suggests that loading induces an early- to- moderate OA pathology by day 15 which generally agrees with previous global Mankin scores of approximately 4 on a 10-point grading scale for this model[25]. Accordingly, the pericellular width analysis generally corroborates with our previous categorization of the tunable overloading model producing *early* indications of progressive structural degradation.

Previous studies using global Mankin scoring of the TMJ cartilage structure found that overall changes (measured via overall GAG, proteoglycan, and collagen content) were evident at day 15 only in TMJs exposed to 3.5N loading[25]. However, the presented pericellular Mankin sub-scoring suggests there were no evident changes in the pericellular region between loading groups (Figure 6). Investigation of PCM-specific markers reveals pericellular microstructural changes and pericellular reorganization for both loading magnitudes, which were undetected by pericellular Mankin sub-scoring. The collagen VI and aggrecan neo-epitope assays also show change associated with 2N-loading that were not observed by the global Mankin system (Figures 3 & 4). These differences suggest that individual pericellular matrix markers may provide more details in the structural degradation associated with *early* TMJ-OA and may be a more sensitive detection tool over Mankin scoring to distinguish structural remodeling of TMJs present in both persistent and resolving symptomatic pain.

This study's use of immunohistochemical evaluation to determine pericellular structural changes in TMJ is limited in several ways. With this approach, it is challenging to accurately assess pericellular remodeling across different depths of heterogenous tissue due to the compacted, fibrous morphology of the TMJ's superficial layers. IHC assays are also limited in demonstrating functional changes in tissue mechanical properties. Since understanding the heterogenous architecture of the TMJ and measuring functional outcomes from tissue overloading are areas of interest, performing Atomic Force Microscopy (AFM) on TMJ fibrocartilage from our model could be a useful future approach to determine mechanical outcomes relative to tissue depth or magnitude of overloading[57–59]. Furthermore, although pain, inflammation, and catabolic factors are upregulated in the 3.5N TMJ loading case on, or prior to, day 8[2, 25,35,36], the findings of this study reveal detailed pericellular microstructural changes within *both* loading conditions at day 15 after the loading period that were previously undetected. Our preliminary assessment indicated no increases in collagen VI expression nor significant changes in pericellular Mankin scoring at day 8 for the more aggressive, 3.5N-loaded condition, which provided rationale to focus on day 15 outcomes (Supplemental Figures 3 and 4). However, additional time course studies for both PCM markers within each pain condition are needed to define the temporal relationships between the onset of pain, inflammation, and catabolic cascades and pericellular structural outcomes. Additional limitations of this study include the differences of immunohistochemical techniques applied for on collagen VI versus aggrecan NITEGE quantification (Supplemental Figure 1) and inherent subjectivity of manual analysis for both pericellular Mankin scoring and pericellular width analysis. Improvements to mitigate

these limitations include standardizing IHC protocols for both pericellular markers and automating pericellular width tabulations to minimize any subjectivity.

In summary, this study bridges previously determined inflammatory and behavioral outcomes of a TMJ overloading model with tunable pain conditions to detailed pericellular structural modulations within TMJ cartilage tissue. Our hypothesis of increased pericellular structural remodeling in painful, overloaded TMJs is accepted since there are increased levels of collagen VI under both loading paradigms and progressively increased aggrecan neo-epitope in the persistent pain condition. Collagen VI and aggrecan NITEGE neo-epitope respond to overloading associated with both resolving or persistent pain expression, but with differing patterns, underscoring the complexities of pericellular structural molecules and the dynamic nature of the PCM region. The increase in collagen VI and aggrecan neo-epitope as well as pericellular width expansion is characteristic of early-to-moderate osteoarthritic development. Unlike studying the tissue matrix surrounding chondrocytes using global stains and pericellular sub-scorings, our investigation highlights the potential importance of assessing the pericellular matrix remodeling with specific markers as it provides more detailed information about tissue outcomes that could be beneficial to the characterization and diagnosis of TMJ-OA.

Supplementary Material

Refer to Web version on PubMed Central for supplementary material.

Acknowledgements:

This project was funded by the Catherine D. Sharpe Foundation, Oral and Maxillofacial Surgery Foundation, Oral and Maxillofacial Surgery Schoenleber Research Fund from the University of Pennsylvania School of Dental Medicine, a training grant from NIH/NIAMS (T32-AR007132), and a grant from the National Science Foundation (#1826202). The study sponsors had no role in study design, collection, analysis and interpretation of data; in the writing of the manuscript; and in the decision to submit the manuscript for publication. The authors would like to extend thanks to University of Pennsylvania’s Center for Musculoskeletal Diseases and Penn Microscopy Core for training and equipment use.

References

1. Praveena K, Rathika R, Easwaran M, Easwaran B. 2014. Temperomandibular disorders Clinical and Modern Method In Differential Diagnosis. IOSR Journal of Dental and Medical Sciences (IOSR-JDMS). 13(9): 1–7.
2. Kartha S, Zhou T, Granquist EJ, Winkelstein BA. 2016. A rat model of tunable TMJ pain, inflammation & condylar degeneration. Journal of Oral & Maxillofacial Surgery. 74(1):54. e1–e10. [PubMed: 26433038]
3. Wadhwa S, Kapila S. 2008. TMJ disorders: future innovations in diagnostics and therapeutics. Journal of Dental Education. 72(8):930–947. [PubMed: 18676802]
4. Das SK. TMJ osteoarthritis and early diagnosis. 2013. Journal of Oral Biology and Craniofacial Research. 3(3):109–110. [PubMed: 25737896]
5. Wang XD, Zhang JN, Gan YH, Zhou YH. 2015. Current Understanding of Pathogenesis and Treatment of TMJ Osteoarthritis. Journal of Dental Research. 94(5): 666–673. [PubMed: 25744069]
6. Yount K. 2011. Osteoarthritis of the Temporomandibular Joint. Practical Pain Management. 3(4).
7. Chantaracherd P, John MT, Hodges JS, Schiffman EL. 2015. Temporomandibular joint disorders’ impact on pain, function, and disability. Journal of Dental Research. 94(3): 79–86.

8. Stegenga B, de Bont LG, Boering G. 1989. Osteoarthrosis as the cause of craniomandibular pain and dysfunction: A unifying concept. Journal of Oral & Maxillofacial Surgery. 47(3): 249–256. [PubMed: 2646405]

9. Tanaka E, Detamore MS, Mercuri LG. 2008. Degenerative Disorders of the Temporomandibular Joint: Etiology, Diagnosis, and Treatment. Journal of Dental Research, 87(4), 296–307. [PubMed: 18362309]

10. Madden R, Han SK, Herzog W. 2013. Chondrocyte deformation under extreme tissue strain in two regions of the rabbit knee joint. Journal of Biomechanics. 46(3):554–560. [PubMed: 23089458]

11. Ngyuyen BV, Wang Q, Kuiper NJ, et al. 2009. Strain-dependent viscoelastic behaviour and rupture force of single chondrocytes and chondrons under compression. Biotechnology Letters, 31(6): 803–809. [PubMed: 19205892]

12. Guilak F, Ratcliffe A, Mow AC. 1995. Chondrocyte deformation and local tissue strain in articular cartilage: a confocal microscopy study. Journal of Orthopaedic Research. 13(3): 410–421. [PubMed: 7602402]

13. Choi JB, Youn I, Cao L, et al. 2007. Zonal changes in the three-dimensional morphology of the chondron under compression: the relationship among cellular, pericellular, and extracellular deformation in articular cartilage. Journal of Biomechanics. 40(12): 2596–2603. [PubMed: 17397851]

14. Cescon M, Gattazzo F, Chen P, Bonaldo P. 2015. Collagen VI at a glance. Journal of Cell Science. 128: 3525–3531. [PubMed: 26377767]

15. Guilak F, Alexopoulos LG, Uptom ML, et al. 2006. The pericellular matrix as a transducer of biomechanical and biochemical signals in articular cartilage. Annals of the New York Academy of Science. 1068:498–512.

16. Iozzo RV, Schaefer L. 2015. Proteoglycan form and function: A comprehensive nomenclature of proteoglycans. Matrix Biology. 42: 11–55. [PubMed: 25701227]

17. Dean D, Han L, Grodzinsky AJ, Ortiz C. 2006. Compressive nanomechanics of opposing aggrecan macromolecules. Journal of Biomechanics. 39(14): 2555–2565. [PubMed: 16289077]

18. Seog J, Dean D, Plaas AHK, et al. 2002. Direct measurement of glycosaminoglycan intermolecular interactions via high-resolution force spectroscopy. Macromolecules. 35(14): 5601–5615.

19. Buschmann MD, Grodzinsky AJ. 1995. A molecular model of proteoglycan associated electrostatic forces in cartilage mechanics. Journal of Biomechanical Engineering. 117(2): 179–192. [PubMed: 7666655]

20. Khoshgoftar M, Torzilli P, Maher S. 2017. Influence of the pericellular and extracellular matrix structural properties on chondrocyte mechanics. Journal of Orthopedic Research. 36(2): 721–729.

21. Guilak F, Nims RJ, Dicks A, et al. 2018. Osteoarthritis as a disease of the cartilage pericellular matrix. Matrix Biology. 71–72: 40–50.

22. Pauli C, Whiteside R, Heras FL, et al. 2012. Comparison of Cartilage histopathology assessment systems on knee joints at all stages of osteoarthritis development. Osteoarthritis & Cartilage. 20(6): 476–485. [PubMed: 22353747]

23. Xu L, Polur I, Lim C, et al. 2009. Early-onset osteoarthritis of mouse temporomandibular joint induced by partial discectomy. Osteoarthritis & Cartilage. 17(7): 917–922. [PubMed: 19230720]

24. Shen P, Jiao Z, Zheng JS, et al. 2015. Injecting vascular endothelial growth factor into the temporomandibular joint induces osteoarthritis in mice. Scientific Reports. 5: 16244. [PubMed: 26531672]

25. Sperry MM, Yu Y, Welch R. 2018. Grading facial expression is a sensitive means to detect grimace differences in orofacial pain in a rat model. Scientific reports. 8: 13894. [PubMed: 30224708]

26. Van der Slujis JA, Geesink RJ, van der Linden AJ. 1992. The reliability of the Mankin score for osteoarthritis. Journal of Orthopedic Research. 10(1): 58–61.

27. Hambach L, Neureiter D, Zeiler G. 1998. Severe disturbance of the distribution and expression of type VI collagen chains in osteoarthritic articular cartilage. Arthritis and Rheumatology. 41(6): 986–996.

28. Pullig O, Weseloh G, Swoboda B. 1999. Expression of type VI collagen in normal and osteoarthritic human cartilage. Osteoarthritis and Cartilage. 7(2): 191–202. [PubMed: 10222218]

29. Chu WC, Zhang S, Sng TJ, et al. 2017. Distribution of pericellular matrix molecules in the temporomandibular joint and their chondroprotective effects against inflammation. International Journal of Oral Science. 9(1):43–52. [PubMed: 28282029]
30. Peters HC, Otto TJ, Enders JT, et al. 2011. The protective role of the pericellular matrix in chondrocyte apoptosis. Tissue Engineering Part A. 17(15–16): 2017–2024. [PubMed: 21457093]
31. Hardingham T, Fosang A. 1992. Proteoglycans: many forms and many functions. The FASEB Journal. 6(3): 861–870. [PubMed: 1740236]
32. Roughley PJ, Mort JS. 2014. The role of aggrecan in normal and osteoarthritic cartilage. Journal of Experimental Orthopedics. 1(1): 8.
33. Zelenski NA, Leddy HA, Sanchez-Adams J, et al. 2015. Type VI Collagen Regulates Pericellular Matrix Properties, Chondrocyte Swelling, and Mechanotransduction in Mouse Articular Cartilage. Arthritis and Rheumatology. 67(5):1286–1294. [PubMed: 25604429]
34. Alexopoulos LG, Youn I, Bonaldo P, Guilak F. 2009. Developmental and osteoarthritic changes in Col6a1-knockout mice: biomechanics of type VI collagen in the cartilage pericellular matrix. Arthritis and Rheumatology. 60(3): 771–779.
35. Sperry MM, Stiansen N, Ghimire P, et al. 2018. Repeated, painful jaw overloading activates osteoclasts & remodels the trabecular architecture of the TMJ condyle. 8th World Congress of Biomechanics Conference Proceeding.
36. Sperry MM, Yu YH, Kartha S, et al. 2020. Intra-articular etancercept attenuates pain and hypoxia from TMJ loading in the rat. Journal of Orthopedic Research. DOI: 10.1002/jor.24581.
37. Institute for Laboratory Animal Research. Guide for the care and use of laboratory animals: 8th Ed. Guide for the Care and Use of Laboratory Animals, https://doi.org/10.2307/1525495, https://grants.nih.gov/grants/olaw/guide-for-the-care-and-use-of-laboratory-animals.pdf (2011).
38. Zimmermann M. 1983. Ethical guidelines for investigations of experimental pain in conscious animals. Pain. 16(2): 109–110. [PubMed: 6877845]
39. Nicoll SB, Hee CK, Davis MB, et al. 2010. A rat model of temporomandibular joint pain with histopathologic modifications. J Orofac Pain 24: 298. [PubMed: 20664832]
40. Zhang L, Hu J, Athanasiou KA. 2009. The role of tissue engineering in articular cartilage repair and regeneration. Critical Reviews Biomedical Engineering. 37(1–2):1–57
41. Dreier R. 2010. Hypertrophic differentiation of chondrocytes in osteoarthritis. The developmental aspect of degenerative joint disorders. Arthritis Research & Therapy. 12(5): 216. [PubMed: 20959023]
42. Embree M, Ono M, Kilts T, et al. 2011. Role of subchondral bone during early-stage experimental TMJ osteoarthritis. Journal of Dental Research. 90(11):1331–1338. [PubMed: 21917603]
43. Kuroda S, Tanimoto K, Izawa T, et al. 2009. Biomechanical and biochemical characteristics of the mandibular condylar cartilage. Osteoarthr. Cartil 17(11):1408–1415 Available from: 10.1016/j.joca.2009.04.025.
44. Phillips E et al. 2019. Biomimetic proteoglycans diffuse throughout articular cartilage and localize within the pericellular matrix. Journal of Biomedical Materials Research. 107(9): 1977–1987. [PubMed: 31056821]
45. Nugent A, Speicher D, Gradisar I, et al. 2009. Advanced Osteoarthritis in Humans is Associated with Altered Collagen VI Expression and Upregulation of ER-stress Markers Grp78 and Bag-1. Journal of Histochemistry & Cytochemistry. 57(10): 923–931. [PubMed: 19546472]
46. Janusz MJ, Little CB, King LE, et al. 2004. Detection of aggrecanase- and MMP-generated catabolic neoepitopes in the rat iodoacetate model of cartilage degeneration. Osteoarthritis and Cartilage. 12(9): 720–728. [PubMed: 15325638]
47. Nagase H, Kashiwagi M. 2003. Aggrecanases and cartilage matrix degradation. Arthritis Research & Therapy. 5(2):94–103. [PubMed: 12718749]
48. Ghassemi-Nejad S, Kobezda T, Rauch TA, et al. 2011. Osteoarthritis-like damage of cartilage in the temporomandibular joints in mice with autoimmune inflammatory arthritis. Osteoarthritis & Cartilage. 19(4):458–465. [PubMed: 21262368]
49. van Meurs JB, van Lent PL, Holthuysen AE, et al. 2001. Kinetics of aggrecanase- and metalloproteinase-induced neoepitopes in various stages of cartilage destruction in murine arthritis. Arthritis and Rhumatology, 42(6): 1128–1139.

50. Tortorella M, Pratta M, Fox J, Arner E. 1998. The Interglobular Domain of Cartilage Aggrecan Is Cleaved by Hemorrhagic Metalloproteinase HT-d (Atrolysin C) at the Matrix Metalloproteinase and Aggrecanase Sites. The Journal of Biological Chemistry. 273: 5846–5850. [PubMed: 9488721]

51. Leonardi R, Crimi S, Almeida LE, et al. 2015. ADAMTS-4 and ADAMTS-5 expression in human temporomandibular joint discs with internal derangement, correlates with degeneration. Journal of Oral Pathology & Medicine. 44(10): 870–875. [PubMed: 25477257]

52. Fujita H, Morisugi T, Tanaka Y, et al. 2009. MMP-3 activation is a hallmark indicating an early change in TMJ disorders, and is related to nitration. International Journal of Oral & Maxillofacial Surgery. 38(1): 70–78. [PubMed: 19117728]

53. Poole CA. 1997. Articular cartilage chondrons: form, function, and failure. Journal of anatomy. 191(1): 1–13. [PubMed: 9279653]

54. Embry Flory JJ, Fosang AJ, Knudson W. 2006. The accumulation of intracellular ITEGE and DIPEN neoepitopes in bovine articular chondrocytes is mediated by CD44 internalization of hyaluronan. Arthritis and Rheumatology. 54(2):443–454.

55. Yasumoto T, Bird JL, Sugimoto K, et al. 2003. The G1 domain of aggrecan released from porcine articular cartilage forms stable complexes with hyaluronan/link protein. Rheumatology. 42(2): 336–342. [PubMed: 12595632]

56. Lotz MK, Otsuki S, Grogan SP, Sah R, Terkeltaub R, D'Lima D. Cartilage cell clusters. Arthritis Rheum. 2010;62(8):2206–2218. doi:10.1002/art.27528 [PubMed: 20506158]

57. Chery DR et al. Early changes in cartilage pericellular matrix micromechanobiology portend the onset of post-traumatic osteoarthritis. Acta Biomaterialia. 2020; 111: 267–278. doi: 10.1016/j.actbio.2020.05.005 [PubMed: 32428685]

58. Xu X et al. Knockdown of the pericellular matrix molecule perlecan lowers in situ cell and matrix stiffness in developing cartilage. 2016; 418(2): 242–247. doi:10.1016/j.ydbio.2016.08.029.

59. Chandrasekaran P, Doyran B, Li Q, et al. Biomechanical properties of murine TMJ articular disc and condyle cartilage via AFM-nanoindentation. J Biomech. 2017; 60:134–141. doi:10.1016/j.jbiomech.2017.06.031 [PubMed: 28688538]

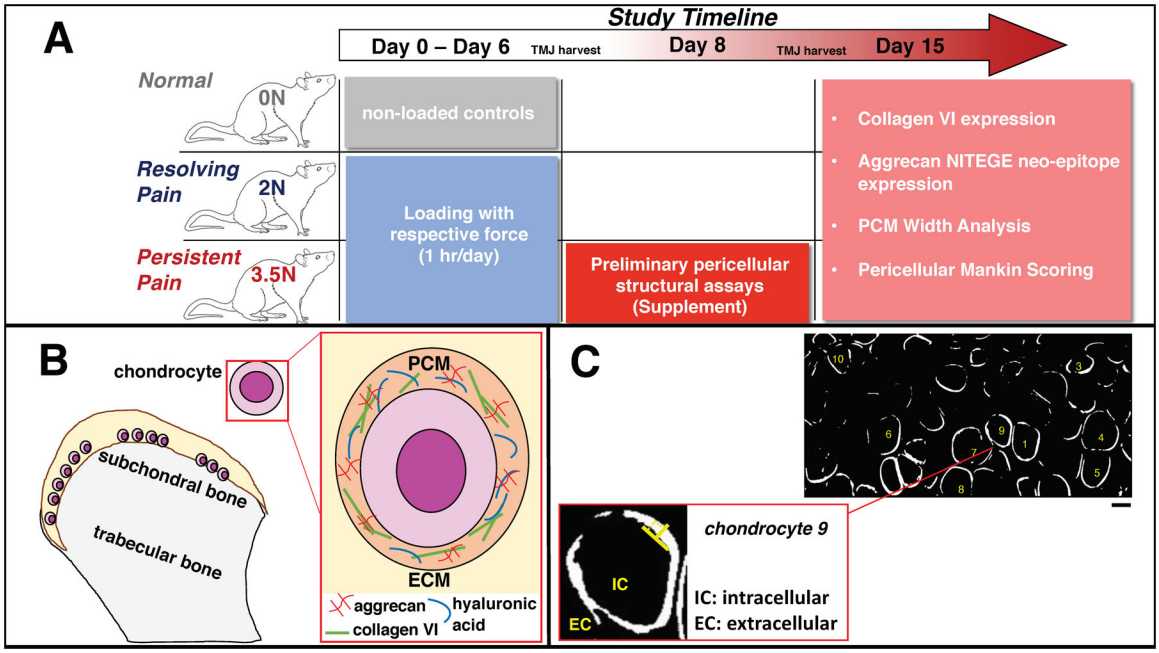

Figure 1. Summarized Methods Panel.

(A) Overview of the study timeline: the repeated loading period occurred from Day 0 to Day 6 to induce tunable pain; an early pericellular structural assessment was performed on harvested TMJs within the 3.5N-loaded group at Day 8; and all experimental groups' pericellular structural assays were completed at Day 15. (B) Illustration of the PCM within TMJ cartilage. Our study focuses on evaluation of collagen VI fibrillar protein and fragments of bottle-brush shaped aggrecan proteoglycan attachments following painful loading. (C) Example image of hypertrophic chondrocytes and measurement technique for pericellular width quantification via collagen VI marker guidance. *(top)* TMJ sections labelled for collagen VI were converted to bifiltered images through MATLAB. 10 randomly selected chondrocytes from each image (2 images per animal) were measured. Location of measurement along the PCM (in white) was also randomly selected. *Scale Bar =10μm. (bottom)* Expanded view of a single chondrocyte displaying inner and outer boundaries and perpendicular direction (⊥) of manual width measurement completed via ImageJ.

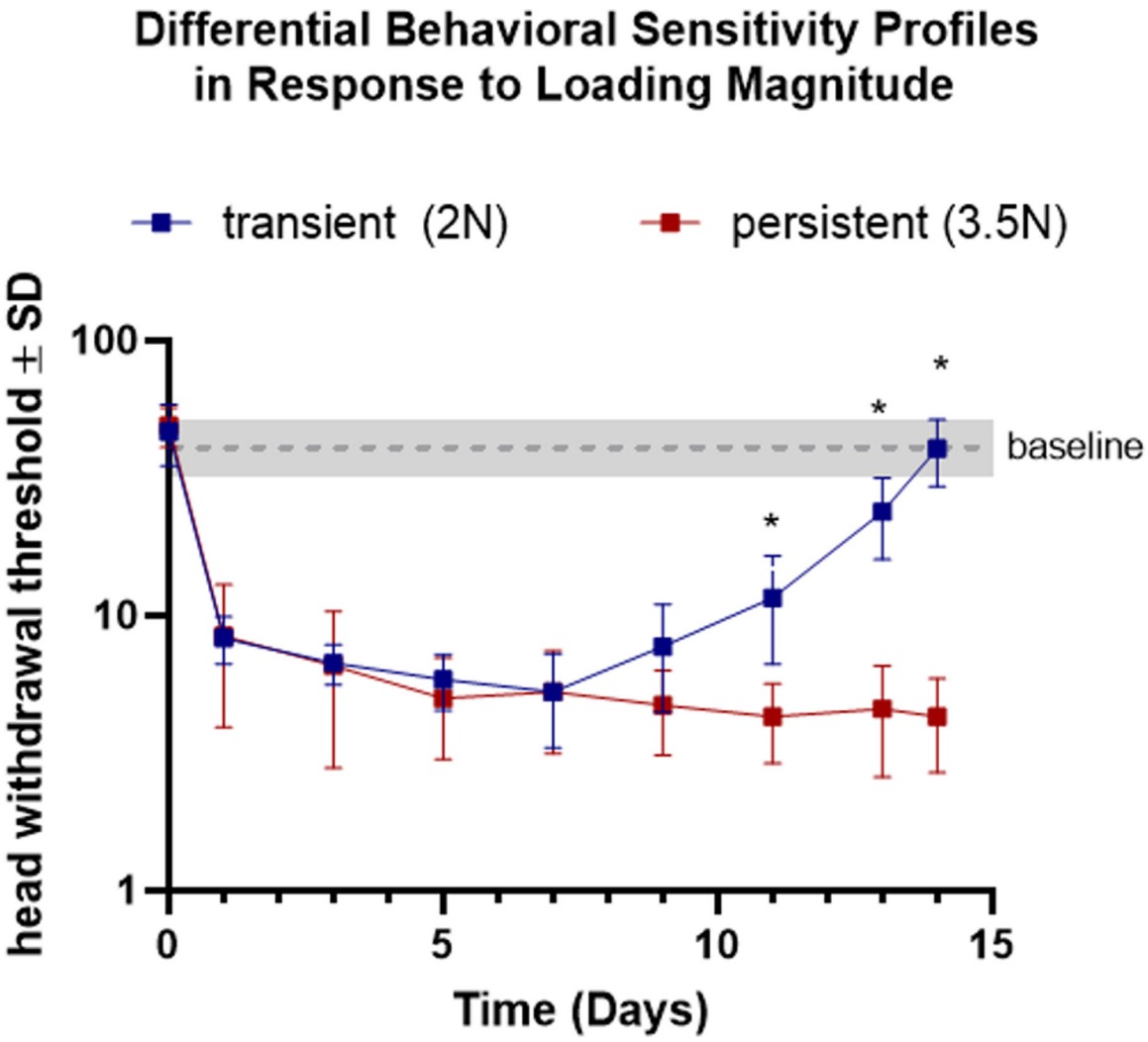

Figure 2. Jaw overloading magnitude corresponds to distinct behavioral sensitivity profiles.
In rats used for the pericellular structural assays (n=7/group), head withdrawal threshold differs between 2N and 3.5N loaded joints on days 11, 13, and 14 (*). The gray line represents the baseline threshold (42.29 ± 7.96) of unloaded, matched animals.

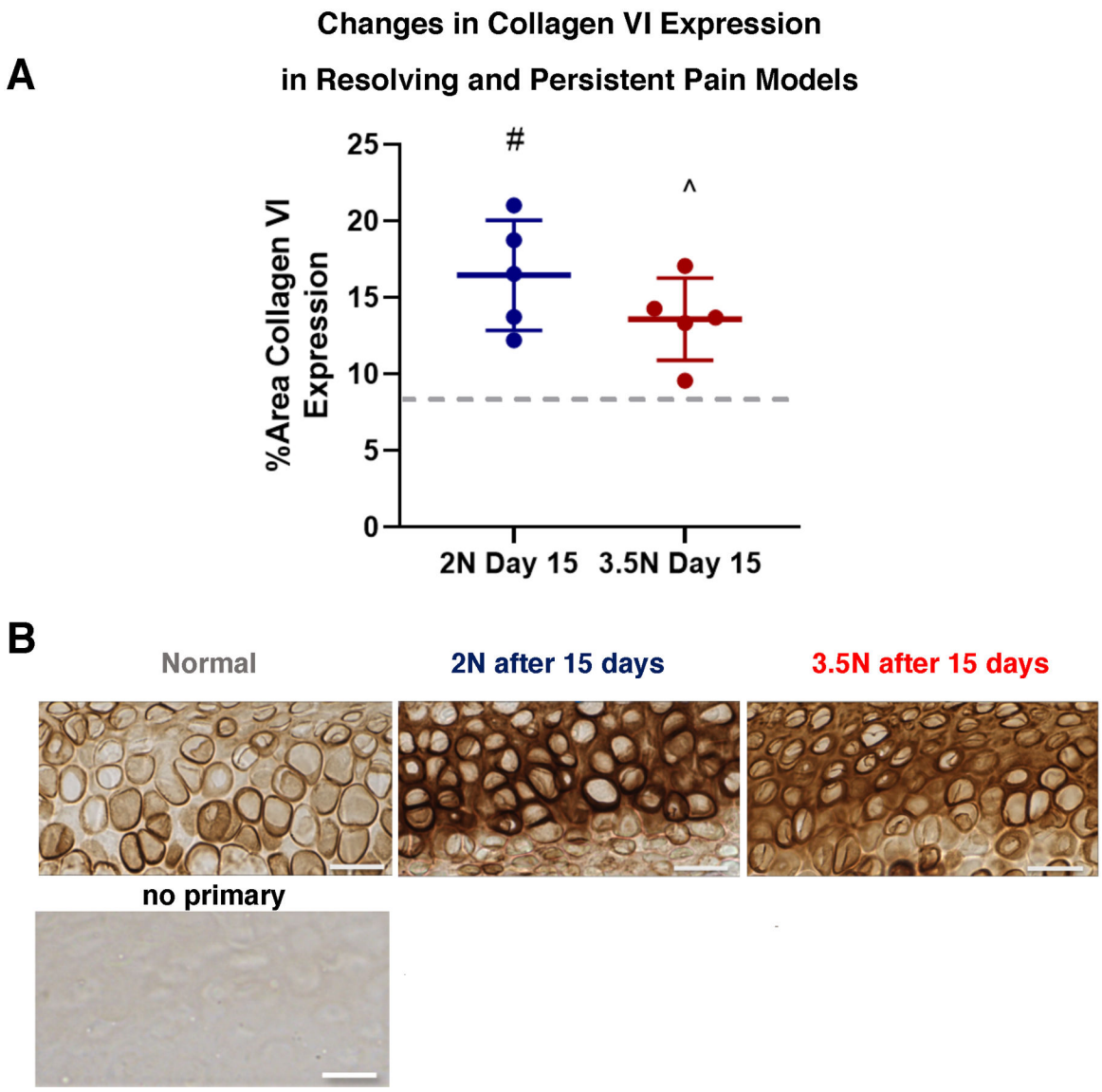

Figure 3. Collagen VI increases similarly in both resolving and persistent models by day 15.

(A) Collagen VI levels increased in both 2N-loaded (#) and 3.5N-loaded samples (^) by day 15 timepoint compared to normal levels (gray dashed line). There was no significant difference between the two day 15 experimental groups, regardless of load magnitude. (B) Corresponding DAB-IHC collagen VI labelling of hypertrophic chondrocytes acquired from normal versus resolving and persistent TMJ pain models. Compared to normal controls, both day 15 groups have dark collagen VI pericellular labelling and diffuse expression into the interterritorial region of the tissue matrix. *Scale bar = 25μm.*

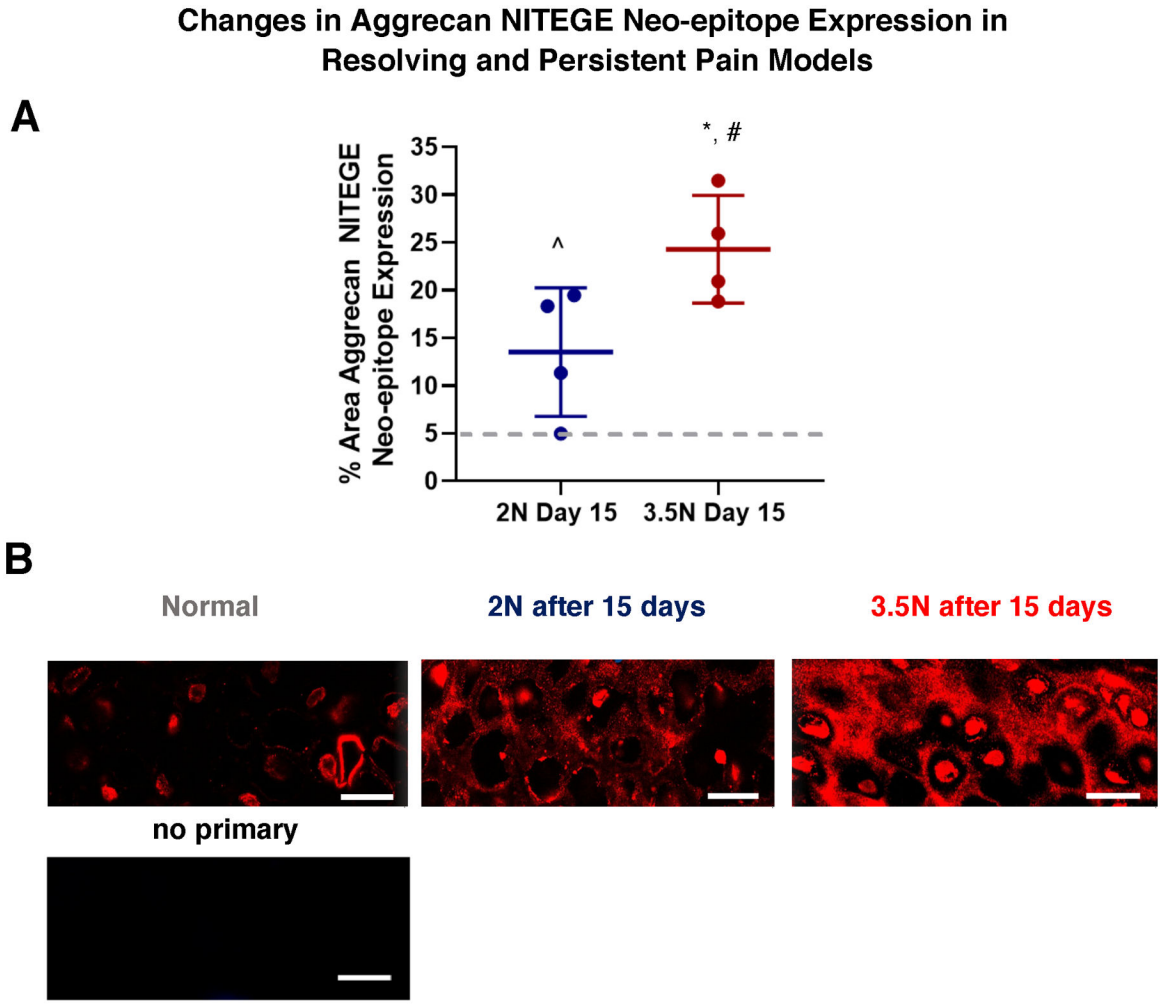

Figure 4. Aggrecan NITEGE neo-epitope expression gradually and directly increases depedent on load magnitude.

(A) Aggrecan neo-epitope increased in both 2N-loaded (^) and 3.5N-loaded (*) TMJs on day 15 over normal (represented by gray dashed line). Additionally, cleaved aggrecan expression was greater in 3.5N over 2N loaded TMJs at day 15 timepoint (#).

(B) Corresponding IF images of aggrecan NITEGE neo-epitope labelled hypertrophic chondrocytes. Compared to normal, unloaded samples, where NITEGE is lightly labelled in the pericellular region and confined locally to the cell, the day 15 loaded samples had increased darkness of label in the pericellular and interterritorial regions of the tissue matrix. The day 15, 3.5N-loaded samples of the persistent paradigm appear darker with more concentrated NITEGE label in comparison to the day 15, 2N-loaded samples of the resolving model. *Scale bar = 15μm.*

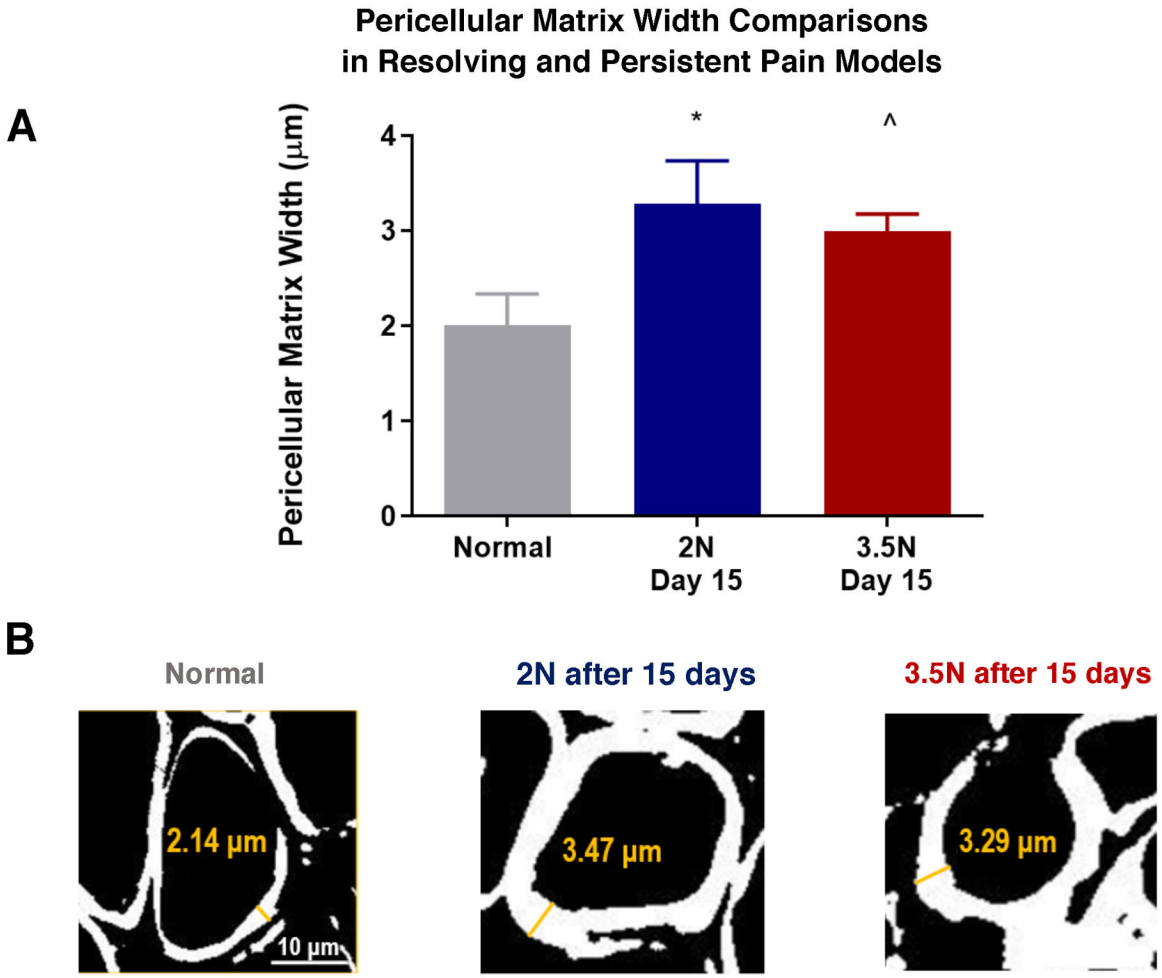

Figure 5. Pericellular width of TMJ chondrocytes expands following 2N or 3.5N loading at day 15.

(A) PCM width for 3.5N-loaded TMJs and 2N-loaded TMJs both indicated expansion of pericellular region over normal (^p=0.002 and *p<0.001 respectively) by the day 15 time point. Both experimental groups averaged approximately 3μm versus normal baseline of 2μm. (B) Representative bi-filtered images used for pericellular width measurements with thickening of collagen VI guidance marker in both loading paradigms at day 15 compared to normal controls. *Scale bar = 10μm.*

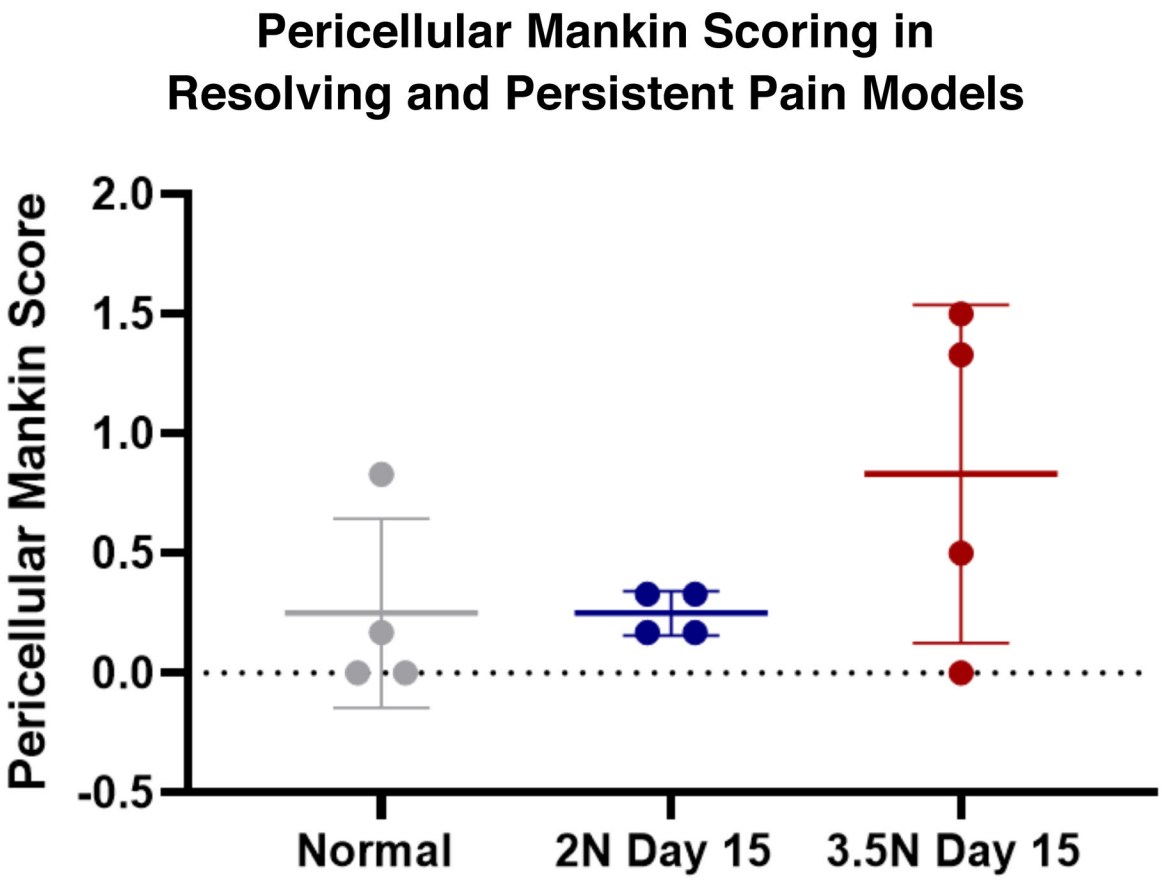

Figure 6. Pericellular Mankin sub-scoring does not detect changes either resolving or persistent pain models at day 15.

Unlike the previously reported global Mankin score findings which detected macrostructural change within 3.5N loaded TMJs at day 15[25], the pericellular Mankin sub-scoring did not detect any significant changes amongst experimental groups and compared to unloaded controls.

Table 1.

Summary of pericellular structural assays and examined conditions.

Assessment	Day 8	Day 15
Collagen VI (n=5/group)	3.5N (Supplemental Figure 3)	2N, 3.5N
Aggrecan Neo-epitope (n=4/group)	---	2N, 3.5N
Pericellular Width Analysis (n=5/group)	---	2N, 3.5N
Pericellular Mankin Scoring (n=4/group)	3.5N (Supplemental Figure 4)	2N, 3.5N